Copyright WILEY-VCH Verlag GmbH & Co. KGaA, 69469 Weinheim, Germany, 2017.

ADVANCED ENERGY MATERIALS

Supporting Information

for *Adv. Energy Mater.,* DOI: 10.1002/aenm.201700012

Molecular Engineered Hole-Extraction Materials to Enable Dopant-Free, Efficient p-i-n Perovskite Solar Cells

Huanle Chen, Weifei Fu, Chuyi Huang, Zhongqiang Zhang, Shuixing Li, Feizhi Ding, Minmin Shi, Chang-Zhi Li, Alex K.-Y. Jen,* and Hongzheng Chen**

Supplementary Data

Molecular Engineered Hole-Extraction Materials to Enable Dopant-Free, Efficient p-i-n Perovskite Solar Cells

Huanle Chen[1†], Weifei Fu[1†], Chuyi Huang[1], Zhongqiang Zhang[1], Shuixing Li[1], Feizhi Din[3], Minmin Shi[1], Chang-Zhi Li[1],* Alex K.-Y. Jen[1,2]* and Hongzheng Chen[1]*

H. Chen, Dr. W. Fu, C. Huang, Z. Zhang, S. Li, Prof. M. Shi, Prof. C.-Z. Li, Prof. A. K.-Y. Jen, Prof. H. Chen

[1]State Key Laboratory of Silicon Materials, MOE Key Laboratory of Macromolecular Synthesis and Functionalization, and Department of Polymer Science and Engineering, Zhejiang University, Hangzhou 310027, P. R. China.
E-mail: czli@zju.edu.cn, hzchen@zju.edu.cn

[2]Prof. A. K.-Y. Jen
Department of Physics and Materials Science, City University of Hong Kong, Kowloon, HK
E-mail: alexjen@cityu.edu.hk

[3]Dr. F. Ding
Division of Chemistry and Chemical Engineering, California Institute of Technology, Pasadena, CA 91125, USA

Experimental Section

Materials. All the chemicals were purchased from Aldrich, ENERGY and TCI Chemical Co. and used as received without further purification.

Instrument. ^{1}H NMR and ^{13}C NMR spectra were recorded on a Bruker Advance III 400 (400 MHz) nuclear magnetic resonance spectroscope. All the data are given as chemical shifts in δ (ppm). MALDI-TOF MS spectra were measured on a Walters Maldi Q-TOF Premier mass spectrometry. UV-vis absorption spectra were taken on a Shimadzu UV-2450 spectrophotometer. Elemental analyses were conducted on a Flash EA 1112 elemental analyzer. Thermogravimetric analysis (TGA) was carried out on a WCT-2 thermal balance under protection of nitrogen at a heating rate of 10 °C min^{-1}. Differential scanning calorimetry (DSC) was recorded on a Perkin-Elmer Pyris 1 differential scanning calorimeter. Cyclic voltammetry (CV) was done on a CHI 660C electrochemical workstation with a Pt disk, Pt plate and standard calomel electrode (SCE) as the working electrode, counter electrode and reference electrode, respectively, in a 0.1 mol L^{-1} tetrabutylammonium hexafluorophosphate (Bu_4NPF_6) CH_2Cl_2 solution.

Synthetic Route for TPP-OMeTAD and TPP-SMeTAD.

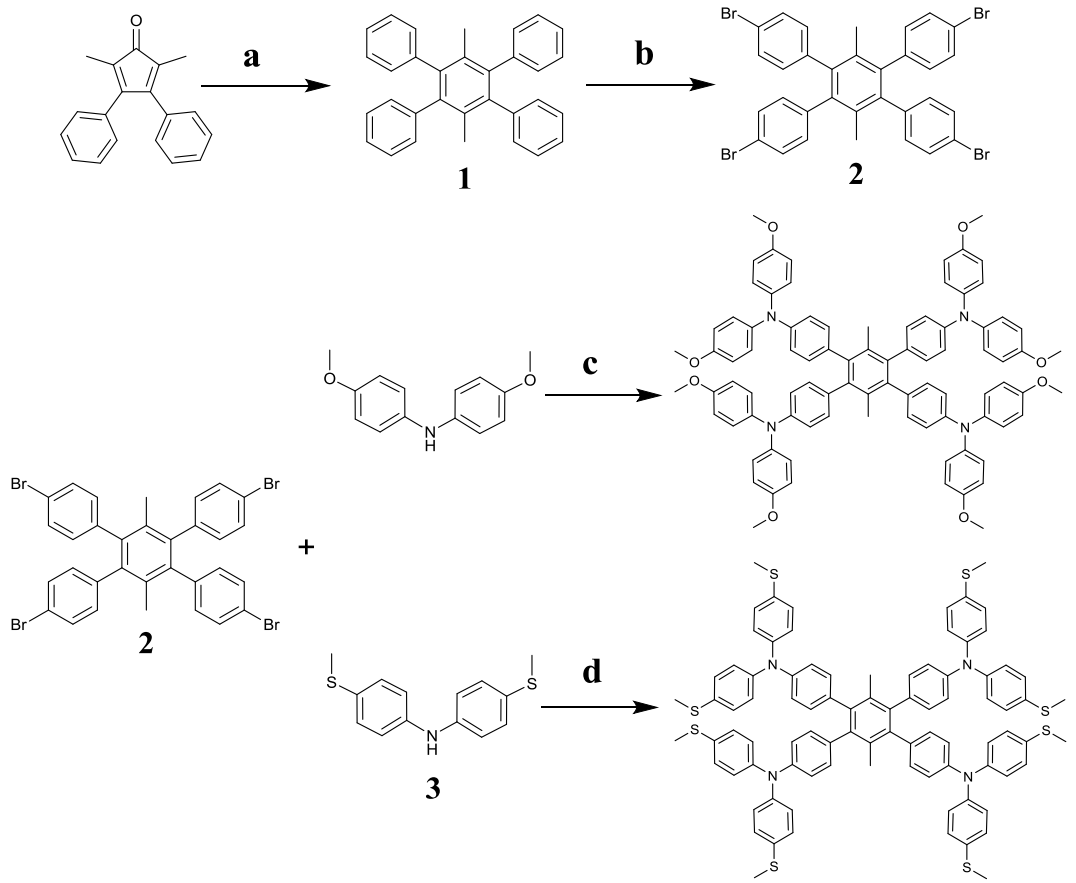

Figure S1 Synthetic routes for HEMs.
(a) diphenylacetylene, diphenyl ether, 140 °C, 67%; (b) bromine, in dark, 24 °C, 45%; (c) $Pd_2(dba)_3$, $P(t\text{-}Bu)_3$, NaOt-Bu, toluene, 100 °C,57%. (d) $Pd_2(dba)_3$, $P(t\text{-}Bu)_3$, NaOt-Bu, toluene, 100 °C,70%.

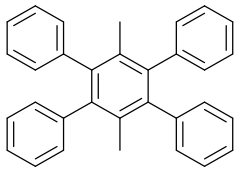

Synthesis of 1,4-dimethyl-2,3,5,6-tetraphenylbenzene.[1] The dimer of 2,5-dimethyl-3,4-diphenylcyclopentadienone (2.00 g, 3.84 mmol) and diphenylacetylene (2.05 g, 11.5 mmol) were dissolved in diphenyl ether (5 mL) and then was heated at reflux for 8 h. Slow cooling yielded crystals after 24 h, which were collected by filtration and washed with hexane. The product was further purified by recrystallization from xylenes, giving 1,4-dimethyl-2,3,5,6-tetraphenylbenzene (1; 2.10 g, 5.11 mmol, 67%) as a colorless

solid: ^{1}H NMR (400 MHz, $CDCl_3$) δ 7.18-7.11 (m, 8H), 7.11-7.03 (m, 12H), 1.80 (s, 6H).

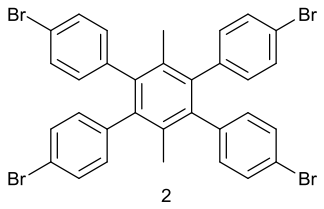

2

Synthesis of 1,4-Dimethyl-2,3,5,6-tetrakis(4-bromophenyl)benzene (2).[1] Powdered tetraphenylethene 1,4-dimethyl-2,3,5,6-tetraphenylbenzene (1.00 g, 2.44 mmol) was treated with bromine (10 ml, 0.2 mol) and the mixture was kept in dark for 24 h at room temp. Ethanol (50 mL) precooled to -78 °C was then added to the reaction flask. The resulting solid was separated by filtration and washed with cold ethanol and then with small portions of 5% (w/v) aqueous $Na_2S_2O_3$. Recrystallization from xylenes and then toluene afforded 1,4-dimethyl-2,3,5,6-tetrakis(4-bromophenyl)benzene (2; 800 mg, 1.21 mmol, 45%) as a white solid. ^{1}H NMR (400 MHz, CDCl3) δ 7.30 (d, J = 8Hz, 8H), 6.87 (d, J = 8Hz, 8H), 1.75-1.71 (m, 6H).

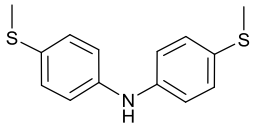

3

Synthesis of bis(4-(methylthio)phenyl)amine (3). To a Schlenk flask, 4-bromoanisole (1.00g, 4.93mmol), p-anisidine (400 mg, 5.42mmol) and sodium tert-butoxide (2.84 g, 29.5mmol) were added and replaced with dry N_2 for three times. 25 ml of degassed anhydrous toluene was added. The mixture was frozen by liquid nitrogen, followed by three times of successive vacuum and N_2 fill cycles. $Pd_2(dba)_3$ (65 mg, 0.071 mmol) and a solution of tri-tert-butylphosphine in toluene (1 M, 0.28 ml) was added under the protection of N_2, and another three times of successive vacuum and N_2 fill cycles was made. The mixture was

heated to 110 ℃ and stirred for 24 h. After cooling down, the mixture was diluted with CH_2Cl_2 and washed by brine for three times. After removing the solvent, the product was purified using column chromatography (silica gel) with hexane/ethyl acetate (10:1, v/v) as the eluent, affording a yellow solid. The material was further purified by recrystallization by CH_2Cl_2/hexane and yielded a colorless solid (705mg, 54.8%). ^{1}H NMR (400 MHz, DMSO-d_6) δ 8. 22 (s, 1H), 7.24-7.17 (m, 4H), 7.05-6.99 (m, 4H), 2.42 (s, 6H).

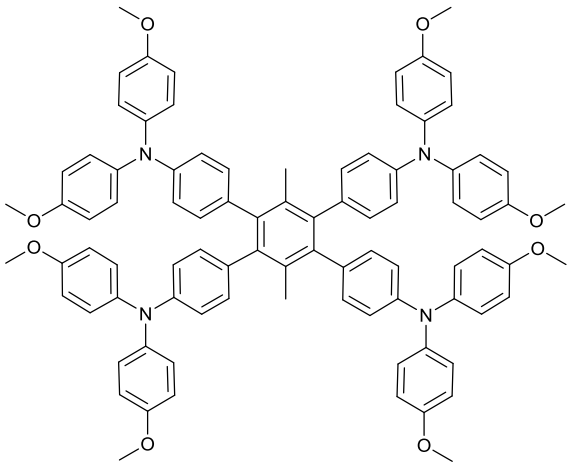

4

Synthesis of 4',5'-bis(4-(bis(4-methoxyphenyl)amino)phenyl)-N4,N4,N4'' (TPP-OMeTAD). To a Schlenk flask, compound 2 (200 mg, 0.28 mmol), di(4-methoxylphenyl) amine (318 mg, 1.38 mmol) and sodium tert-butoxide (160 mg, 1.67 mmol) were added and replaced with dry N_2 for three times. 10 ml of degassed anhydrous toluene was added. The mixture was frozen by liquid nitrogen, followed by three times of successive vacuum and N_2 fill cycles. $Pd_2(dba)_3$ (7.62 mg, 0.008 mmol) and a solution of tri-tert-butylphosphine in toluene (1 M, 0.04 ml) were added under the protection of N_2, and another three times of successive vacuum and N_2 fill cycles was made. The mixture was heated to 110 ℃ and stirred for 36 h. After cooling down, the mixture was diluted with CH_2Cl_2 and washed by brine for three times. After removing the solvent, the product was

purified using column chromatography (silica gel) with hexane/ethyl acetate (10:1~5:1, v/v) as the eluent, affording a white solid. The material was further purified by recrystallization by CH_2Cl_2/hexane before the usage as HEM in perovskite devices and yielded a white solid (210mg, 57%). ^{1}H NMR (400 MHz, Methylene Chloride-d_2) δ 7.49-6.38 (m, 48H), 3.75 (s, 24H), 1.98 (s, 6H). $C_{88}H_{78}N_4O_8$ [M^+] Exact Mass = 1319.61, MS (MALDI-TOF) = 1320.304.

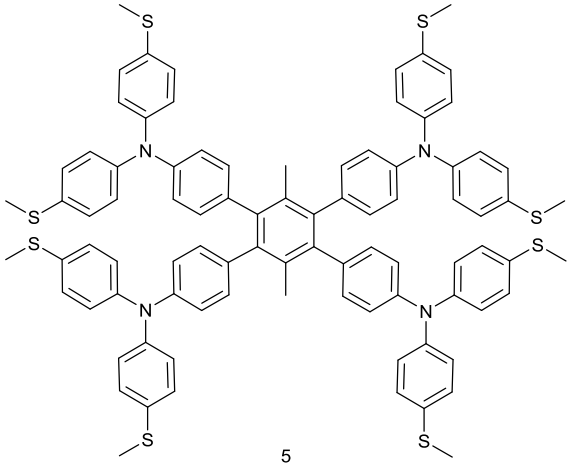

5

Synthesis of 4',5''-bis(4-(bis(4-(methylthio)phenyl)amino)phenyl)-3',6''-dimethyl-N4,N4,N4'' (TPP-SMeTAD). To a Schlenk flask, compound 2 (182 mg, 0.25 mmol), compound 3 (330 mg, 1.26 mmol) and sodium tert-butoxide (146 mg, 1.52 mmol) were added and replaced with dry N_2 for three times. 10 ml of degassed anhydrous toluene was added. The mixture was frozen by liquid nitrogen, followed by three times of successive vacuum and N_2 fill cycles. $Pd_2(dba)_3$ (10 mg, 0.008 mmol) and a solution of tri-tert-butylphosphine in toluene (1 M, 0.04 ml) were added under the protection of N_2, and another three times of successive vacuum and N_2 fill cycles was made. The mixture was heated to 110 °C and stirred for 36 h. After cooling down, the mixture was diluted with CH_2Cl_2 and washed by brine for three times. After removing the solvent, the product was purified using column chromatography (silica gel) with hexane/ethyl

acetate (10:1~5:1, v/v) as the eluent, affording a white solid. The material was further purified by recrystallization by CH_2Cl_2/hexane before the usage as HEM in perovskite devices and yielded a white solid (255 mg, 69.3%). ^{1}H NMR (400 MHz, Methylene Chloride-d_2) δ 7.15-7.13 (m, 16H), 7.01-6.85 (m, 32H), 2.43 (s, 24H), 2.02 (s, 6H). $C_{88}H_{78}N_4S_8$ [M^+] Exact Mass = 1448.10, MS (MALDI-TOF) = 1448.291.

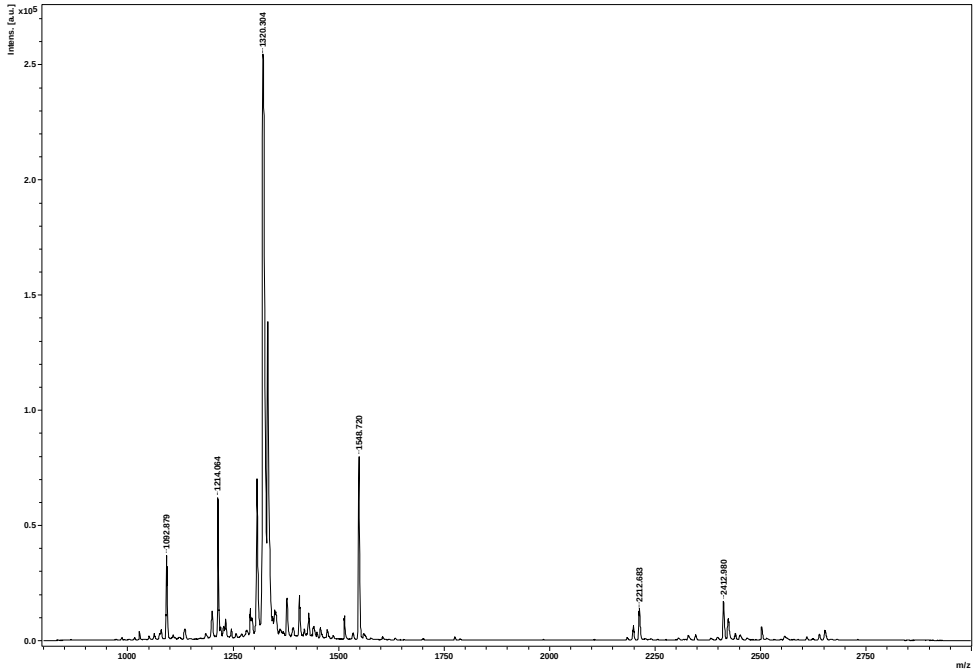

Figure S2 MALDI-TOF Mass spectrum of **TPP-OMeTAD**.

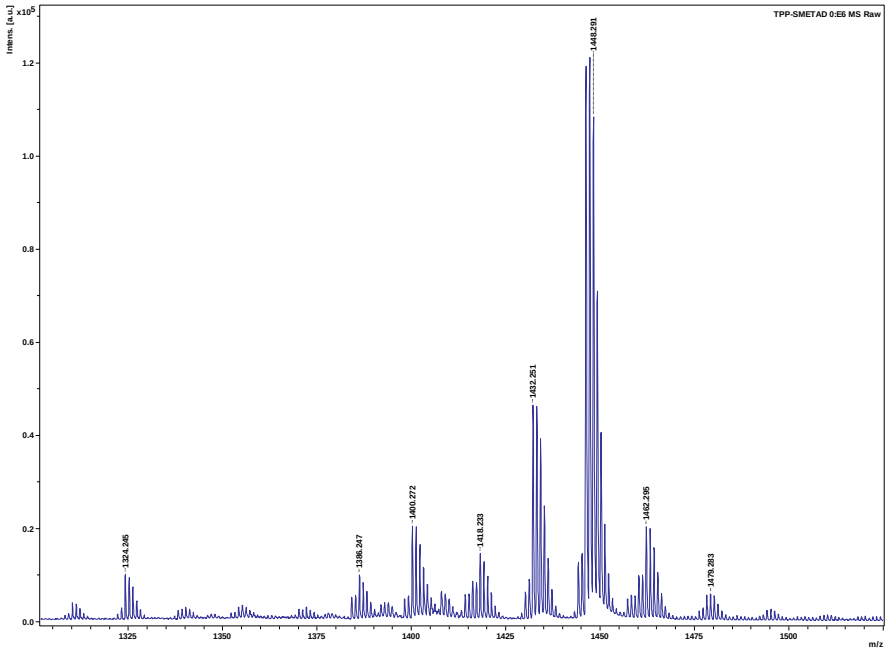

Figure S3 MALDI-TOF Mass spectrum of **TPP-OMeTAD**.

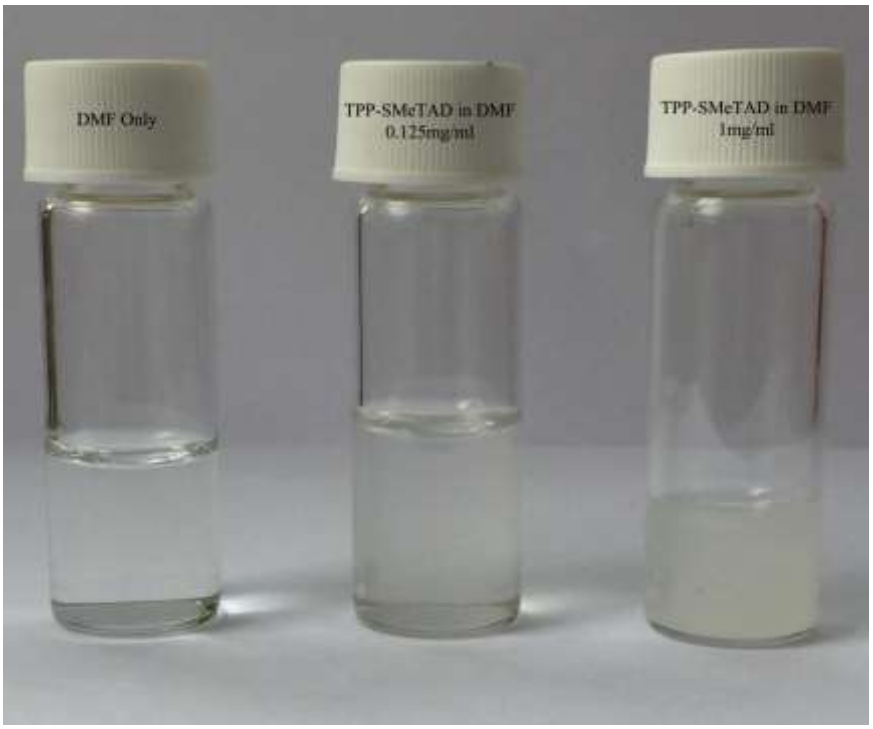

Figure S4 Solubility tests of representative compound, TPP-SMeTAD in DMF.

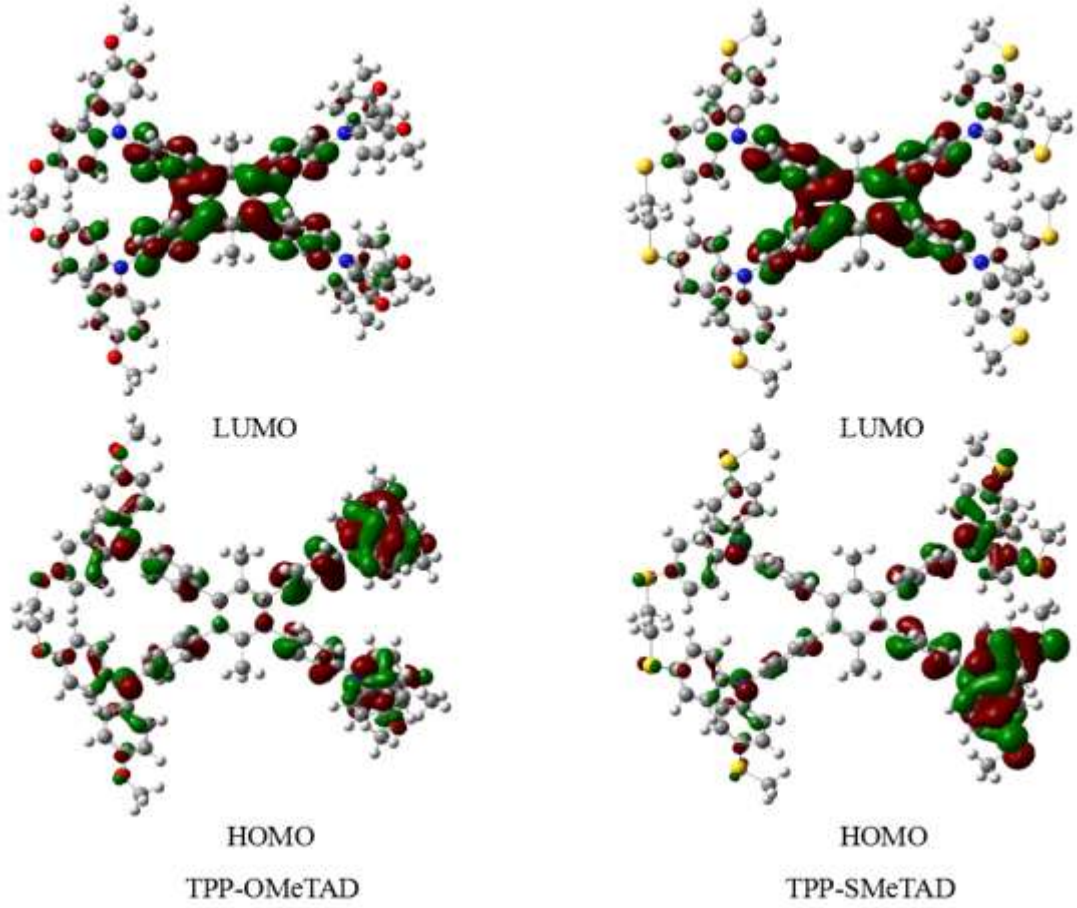

Figure S5 Calculated frontier molecular orbitals of TPP-OMeTAD and TPP-SMeTAD.

Computational details for modeling binding energies

Density functional theory is employed for evaluating the binding energies between the two HEMs with the Pb^{2+} cation. For the sake of computational efficiency, the interaction between the Pb^{2+} cation and the two HEMs is modeled by the interaction of the Pb^{2+} cation with the p-methoxy benzene and p-methylsulfanyl benzene. The binding energies are calculated using the B3LYP hybrid density functional. Two sets of basis functions are used for calibration purposes: the smaller 6-31G*/LanL2DZ basis set (with LanL2DZ effective core potential basis on Pb and 6-31G* all-electron basis on the rest elements), and the larger Def2-TZVP all-electron basis for all elements. The calculated binding energies are summarized in Table

S1 & S2. All geometries are obtained from geometry optimization at the B3LYP/6-31G*/LanL2DZ level of theory. All calculations are performed using the Gaussian 09 quantum chemistry package.[2]

Table S1 Summarized binding energy between Pb^{2+} and atom O.

	Smaller basis 6-31G*//LanL2DZ	Bigger Basis Def2-TZVP
Pb^{2+}	-2.653458388	-192.140379
Ph-O	-346.7648595	-346.907422
Ph-O-Pb^{2+}	-349.6017568	-539.2122458
Bonding energy (kcal/mol)	-115.107924	-103.1890593

Table S2 Summarized binding energy between Pb^{2+} and atom S.

	Smaller basis 6-31G*//LanL2DZ	Bigger Basis Def2-TZVP
Pb^{2+}	-2.653458388	-192.140379
Ph-S	-669.7403841	-669.8838389
Ph-S-Pb^{2+}	-672.5921919	-862.2104512
Bonding energy (kcal/mol)	-124.4642658	-116.8613562[a)]

[a)] The more negative the energy, the stronger the bonding. So, S-Pb^{2+} bond is stronger than O-Pb^{2+} bond.

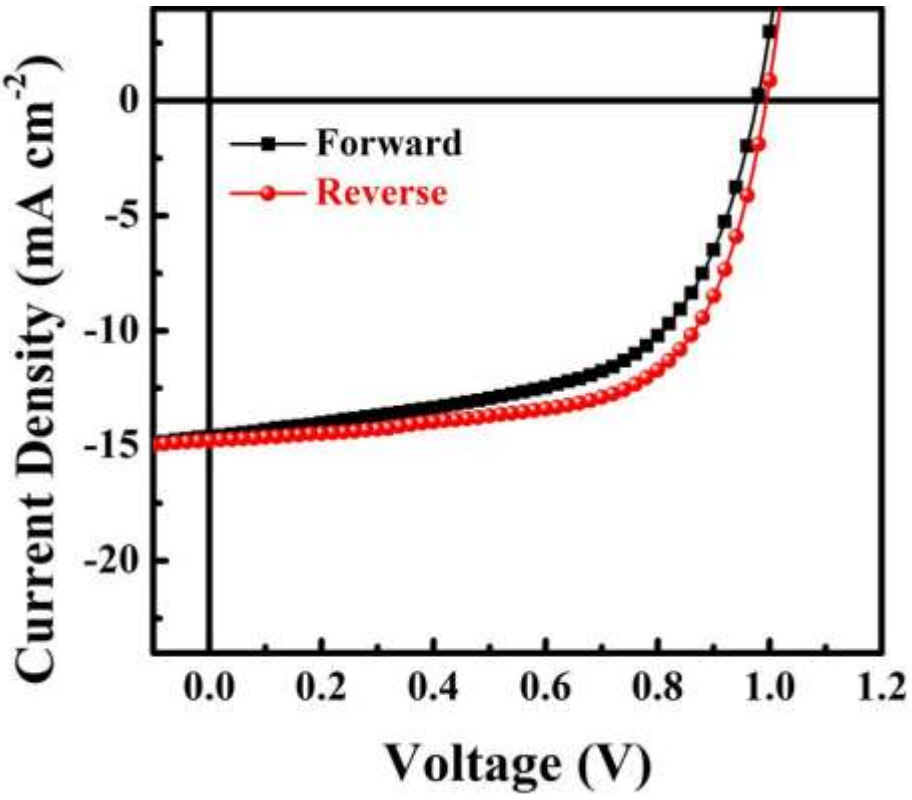

Figure S6 Current-voltage curves and parameters of the $CH_3NH_3PbI_3$ solar cells collected under AM1.5 simulated sun light without any HEM.

Table S3 Performance of the $CH_3NH_3PbI_3$ solar cell without HEM.

HEM	Scan direction	V_{OC} [V]	J_{SC} [mA cm^{-2}]	FF	PCE [%]
w/o	Forward	0.98	14.59	0.59	8.6
	Reverse	0.99	14.77	0.64	9.7

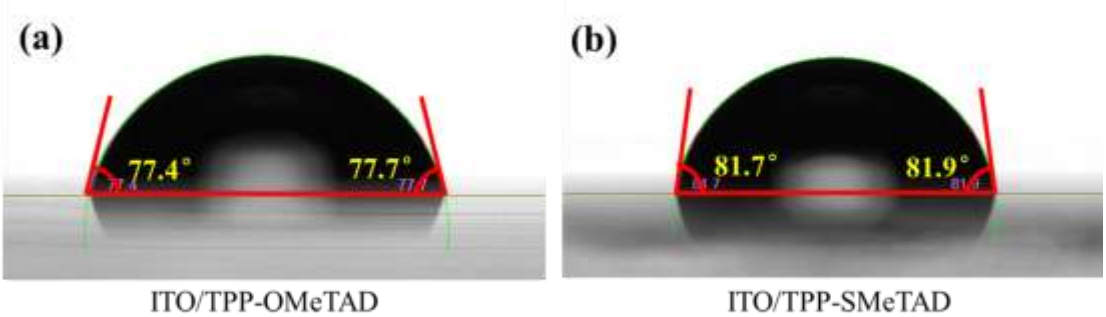

Figure S7 Contact angle of water on (a) **TPP-OMeTAD** and (b) **TPP-SMeTAD**.

Hole Mobility Test

The charge carrier mobility of two HEMs films were measured using the space-charge-limited current (SCLC) method. Hole-only devices were fabricated in a structure of ITO/PEDOT:PSS/TPP-OMeTAD/MoO_3/Al and ITO/PEDOT:PSS/TPP-SMeTAD/MoO_3/Al. The device characteristics were extracted by modeling the dark current under forward bias using the SCLC expression described by the Mott-Gurney law:

Here, $\varepsilon_r \approx 3$ is the average dielectric constant of the film, ε_0 is the permittivity of the free space, μ is the carrier mobility, $L \approx 80$ nm is the thickness of the film, and V is the applied voltage.

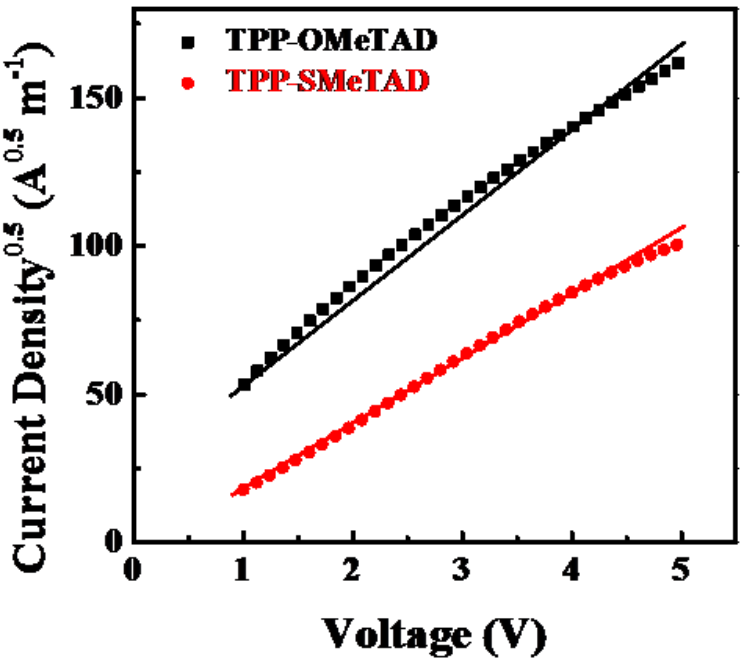

Figure S8 $J^{0.5}$-V curves of hole-only devices with a architecture of ITO/PEDOT:PSS/HEM/MoO_3/Al

Table S4 Summarized hole transport mobilities of different HEMs.

HEM	μ_h [$x10^{-4}$ cm^2 $(v\ s)^{-1}$]
TPP-OMeTAD	1.02±0.19
TPP-SMeTAD	0.74±0.15

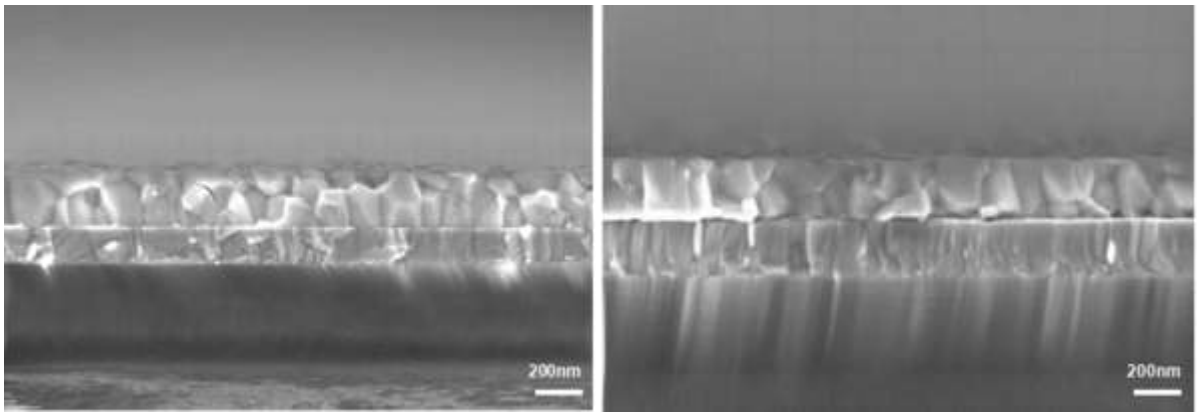

Figure S9 Cross section view of perovskite film fabricated atop of (a) TPP-OMeTAD and (b) TPP-SMeTAD, respectively.

Perovskite Solar Cells Fabrication and *J-V* curves

Materials.

Unless stated otherwise, all materials were purchased from Sigma-Aldrich and used as received. $PC_{61}BM$ was purchased from American Dyes Source, Inc. CH_3NH_3I (MAI) was purchased from Shanghai Materwin New Materials Co. Ltd. ZnO nanoparticles were synthesized by a sol–gel process using Zn acetate and tetramethylammonium hydroxide (TMAH), and dispersed in anhydrous enthanol with a concentration of 20 mg mL^{-1}.[3]

Device fabrication and testing.

Prior to fabrication, the substrates were cleaned by sonication using detergent, deionized water, acetone, and isopropanol sequentially for every 15 min followed by 15 min of ultraviolet ozone (UV-ozone) treatment. The substrates were transferred to a glovebox. TPP-OMeTAD and TPP-SMeTAD films were fabricated by spin-coating a chlorobenzene solution with a concentration of 5 mg mL^{-1} on the ITO substrate and then annealed at 150 °C for 10 min in glove-box.

PbI_2 (1 M) and DMSO (1 M) were dissolved in DMF under stirring at 70 °C. The solution was kept at 70 °C during the whole procedure. The solution was then spin coated on the HEM film at 6000 rpm for 60 s. Then a solution of MAI in 2-propanol (IPA) (50 mg mL^{-1}) was dropped and spin-coated at 6000 rpm for 60 s. Afterwards, the as prepared films were heated at 90°C for 15 min. After cooling down, a layer of [6,6]-phenyl-C_{61}-butyric acid methyl ester ($PC_{61}BM$, 20 mg mL^{-1} in chlorobenzene) was spin-coated at 2000 rpm for 45 s. A hole-blocking layer was deposited *via* spin-coating ZnO nanoparticles in ethanol at 4000 rpm for 30 s on the top of $PC_{61}BM$ layer. Subsequently, samples were loaded into a vacuum deposition chamber (background pressure $\approx 5 \times 10^{-4}$ Pa) to deposit a 100 nm thick Al cathode with a shadow mask. To specify the illuminated area, we used an aperture (shadow mask) with an area of 0.06 cm^2, whereas the total device area defined by the overlap of the electrodes was approximately 0.12 cm^2.

The *J-V* characteristics were measured with Keithley 2400 measurement source units with the devices maintained at room temperature in glove-box. The photovoltaic response was measured under a calibrated solar simulator (Enli Technology) at 100

mW cm^{-2}, and the light intensity was calibrated with a standard photovoltaic reference cell. The EQE spectrum was measured using a QE-R Model of Enli Technology.

References

[1] K. E. Maly, E. Gagnon, T. Maris, J. D. Wuest, *J. Am. Chem. Soc.* **2007**, 129, 4306.

[2] Frisch, M. J.; Trucks, G. W.; Schlegel, H. B.; Scuseria, G. E.; Robb, M. A.; Cheeseman, J. R.; Scalmani, G.; Barone, V.; Mennucci, B.; Petersson, G. A.; et al. *Gaussian Development Version Revision H.13*, Gaussian Inc.: Wallingford, CT, **2010**.

[3] L. Qian, J. H. Yang, R. J. Zhou, A. W. Tang, Y. Zheng, T. K. Tseng, D. Bera, J. G. Xue, P. H. Holloway, *J. Mater. Chem.*, **2011**, 21, 3814.